

Phonon Scattering and Internal Friction in Dielectric and Metallic Films at Low Temperatures

P. D. Vu¹, Xiao Liu², and R. O. Pohl^{3,*}

¹*Department of Physics, Wellesley College, Wellesley, Massachusetts 02481, USA*

²*SFA, Inc., Largo, Maryland 20774, USA*

³*LASSP, Cornell University, Clark Hall, Ithaca, New York 14853-2501, USA*

*email: pohl@ccmr.cornell.edu

(December 2, 2024)

We have measured the heat conduction between 0.05 K and 1.0 K of high purity silicon wafers carrying on their polished faces thin dielectric films of *e*-beam amorphous Si, molecular beam epitaxial (MBE) Si, *e*-beam polycrystalline CaF₂, and MBE CaF₂, and polycrystalline thin metallic films of *e*-beam Al, sputtered alloy Al 5056, *e*-beam Ti, and *e*-beam Cu. Using a Monte Carlo simulation with no free parameters to analyze the conduction measurements, we have determined the phonon mean free path within the films, and found it to be much shorter even than in typical bulk amorphous solids. We have compared these results with the internal friction of these films. We found, however, their internal friction at low temperatures strikingly close to that of amorphous solids, both in magnitude and in their temperature independence, with the exception of the MBE Si and alloy Al 5056, whose internal friction is even much smaller than that of amorphous solids. Thus, the heat conduction measurements do not support the picture that the lattice vibrations of these films are glasslike, as had been surmised earlier for metal films, on the basis of low temperature internal friction measurements alone [Phys. Rev. B **59**, 11767 (1999)]. At the least, the films must contain additional scattering centers which lead to the very small phonon mean free path. Most remarkably, the MBE Si shows the same strong scattering of thermal phonons as do the other films, while having the negligible internal friction expected for a perfect film. The disorder causing the strong scattering of the thermal phonons in this film is completely unknown. The non-glasslike phonon scattering phenomena observed here in thin dielectric and metallic films deserve further investigations.

I. INTRODUCTION

Scientific and technological interest in thin films is vast. In particular, thin films on substrates have many practical uses, such as in microelectronic, magneto-optic, optical, thermal, and photo-voltaic applications [1,2]. It is, therefore, important to characterize such films and compare their properties to those of bulk materials. Moreover, many widely used substances can only be produced in thin film form, like amorphous silicon. Using a technique described previously [3], thermal phonons with wavelengths on the order of 100 to 1000 nm (frequencies on the order of 10 to 100 GHz) have been used here to study disorder in such films, in addition to internal friction and bulk thermal conductivity measurements.

Recently, elastic measurements have shown that crystalline metal films on silicon substrates have a large, nearly temperature independent internal friction plateau at low temperatures, with a magnitude similar to that of amorphous solids [4]. A possible explanation was that crystalline metal films have the same density of tunneling states as amorphous solids. In disordered crystals, such states are called glass-like excitations [5]. The primary motivation at the start of the present investigation was, therefore, to test whether crystalline metal films have

indeed glass-like excitations. According to the tunneling model [6], the tunneling strength which determines the internal friction plateau (caused by relaxational scattering of phonons) also determines the phonon thermal conductivity (caused by resonant scattering of phonons) below ~ 1 K, although the resonantly scattered thermal phonons sample a different part of the tunneling state spectrum [7]. This close connection between the internal friction plateau and the thermal conductivity—the thermal phonon mean free path—has been tested successfully in many cases for bulk amorphous solids [8] as well as for bulk disordered crystals [7], and constitutes a major success of the tunneling model [6]. Using the new technique for studying phonon scattering in thin films, we have recently extended these tests successfully to amorphous silica films [3] and to crystalline silicon layers which had been disordered by ion implantation to the point of amorphization [9].

Here we will apply the same test to an amorphous Si (*a*-Si) film, to several disordered metallic and dielectric crystalline films, and to a crystalline Si film which was produced by molecular beam epitaxy (MBE), and which is therefore expected to contain fewer defects than films produced by other means. We will compare the measured phonon mean free path ($\ell_{\text{film(HC)}}$) as deter-

mined from heat conduction (HC) measurements with the phonon mean free path ($\ell_{\text{film(TM)}}$) as predicted from the internal friction measurements with the aid of the tunneling model (TM). If these two quantities agree with each other, we would have further evidence that these films have glass-like excitations (the ultimate and still missing test being that of a specific heat anomaly varying linearly with temperature [5]). Such evidence would provide further insight into the nature of what is tunneling and how universal this glassy behavior is, and would have significant ramifications for studies involving phonon and/or electron transport, particularly in thin metal films. The vast amount of studies on thin films appear to be controversial in many areas involving electron and/or phonon transport, such as electron-phonon coupling [10,11], dimensional effects and localization [12–14], dislocations [15–18], resistivity [19,20] including the Kondo effect [21–25], and superconductivity [24,26–28]. If glass-like excitations were indeed present in metal films, their effects might be wide ranging in ways not generally appreciated [24].

II. EXPERIMENTAL MATTERS

The thin films were deposited either on Czochralski-grown, n-type with $\sim 2000 \Omega \text{cm}$ resistivity, $\langle 111 \rangle$ oriented, double-side Syton-polished silicon substrates, or on float-zone refined, undoped with $\sim 10 \text{ k}\Omega \text{cm}$ resistivity, $\langle 100 \rangle$ oriented, double-side Syton-polished silicon substrates [29]. The *a*-Si film, the Al, Cu, Ti films, and one CaF₂ film were prepared by *e*-beam evaporation in a standard vacuum, with the substrate held at room temperature. A film of the aluminum alloy Al 5056 (containing, by weight, 5.2% Mg, 0.1% Mn, and 0.1% Cr) was prepared by sputtering in order to preserve its chemical composition, with the substrate also held at room temperature. This alloy was chosen because of its exceptionally small low temperature internal friction even in thin film form [4].

A crystalline Si (*c*-Si) film was produced by MBE on $\langle 100 \rangle$ oriented substrate at Texas Instruments (Dallas) by G. Wilk under UHV conditions and with a substrate temperature of 600°C. Through secondary ion mass spectroscopy (SIMS), R. Reedy at the National Renewable Energy Laboratory (NREL) detected the following chemical elements: boron less than $\sim 10^{16} \text{ cm}^{-3}$, nitrogen $\sim 3 \times 10^{16} \text{ cm}^{-3}$, carbon $\sim 3 \times 10^{17} \text{ cm}^{-3}$, and hydrogen $\sim 2 \times 10^{18} \text{ cm}^{-3}$. These concentrations were similar in the MBE film and the silicon substrate. Only the oxygen contents differed between substrate ($\sim 5 \times 10^{17} \text{ cm}^{-3}$) and film ($\sim 5 \times 10^{18} \text{ cm}^{-3}$). For all these detected impurities, an anneal (500°C, 1 hr followed by 700°C, 1.5 hr) caused no measurable change of their concentrations.

A CaF₂ film was also grown by MBE on $\langle 111 \rangle$ oriented substrate at the University of Georgia (Athens) by K.

Krebs under UHV conditions and a substrate temperature of 750°C. This 400 nm thick film, although probably more highly ordered than an *e*-beam one, is nevertheless expected to contain disorder since the pseudomorphic epitaxial growth is known to break down at film thicknesses exceeding 10 nm [30,31], leading to structural relaxation. Internal stresses are also expected to result from differential thermal contraction as the sample is cooled from the deposition temperature.

All films were found to have a mirror-like finish and to be uniform in color, indicating optical smoothness and uniform thickness. Film thickness was determined by calibrated vibrations of a 6 MHz plano-convex quartz crystal. When possible, it was double-checked with a step surface profiler. Details on the films are contained in Table I.

Thermal phonon mean free paths ($\ell_{\text{film(HC)}}$) were determined between 0.05 and 1.0 K by the technique described in Ref. [3]. Some further details can be found in the Appendix. Thin film internal friction was measured on high purity silicon double-paddle oscillators which have exceptionally small background damping, as detailed in Ref. [4]. The substrates are float-zone refined, undoped with $\sim 10 \text{ k}\Omega \text{cm}$ resistivity, $\langle 100 \rangle$ oriented, double-side Syton-polished. The thermal conductivity of a bulk Al sample (polycrystalline rod, 2.5 mm in diameter and 25.7 mm long) was measured by the standard steady-state four-probe technique after an anneal in vacuum at 560°C followed by plastic deformation at room temperature (stretching in an Instron machine, 5% elongation). Its nominal purity (supplied by Research and PVD Materials Corp., Wayne, NJ) is 99.999% (5N). Its internal friction was measured by E. Thompson at Cornell University using a torsional oscillator (for details, see Ref. [4]).

Prior to mounting for the heat conduction measurements, samples were, when appropriate, either put through an RCA clean [32] or immersed in a hot sulfuric acid solution (1 part H₂O₂ poured into 5 parts H₂SO₄) [33] as a chemical cleaning procedure for removing organic and metallic contaminants. For the internal friction measurements, all films were deposited onto double-paddle oscillators, except for the MBE Si film, which was deposited onto a wafer from which an oscillator was subsequently shaped. This involves the deposition of a low stress silicon-nitride film onto both sides of the wafer. This step was done in the MOS area of the Cornell Nanofabrication Facility and involves heating the wafer to 850°C for 20 minutes. Thus, the internal friction of the MBE Si film was measured only after such a short anneal, while the thermal phonon scattering was measured before and after a longer anneal (500°C, 1 hr followed by 700°C, 1.5 hr). Both the heat conduction and the internal friction measurements were performed on samples carrying *e*-beam *a*-Si films before and after an anneal at 700°C for 1 hr. All the annealing processes

TABLE I. Preparation parameters of the thin films used for the heat conduction measurements in this work. The Cu film has a thin (100Å) adhesive layer of Ti between it and the silicon substrate. The alloy Al 5056 film contains, by weight, 5.2% Mg, 0.1% Mn, and 0.1% Cr. The films were deposited onto either one or both of the wide polished substrate faces (see Ref. [3]), as indicated in the last column. Note for the internal friction measurements, the substrates are always $\langle 100 \rangle$ oriented.

	deposition technique	base pressure (Torr)	substrate temperature (°C)	substrate orientation	deposition rate (Å/s)	film thickness (μm)
α -Si	<i>e</i> -beam	2×10^{-7}	room	$\langle 100 \rangle$	15	0.5, one
MBE Si	MBE	UHV	600	$\langle 100 \rangle$	3	0.4, one
CaF ₂	<i>e</i> -beam	1×10^{-6}	room	$\langle 111 \rangle$	10	0.1, both
MBE CaF ₂	MBE	UHV	750	$\langle 111 \rangle$	0.14-0.28	0.4, one
Al	<i>e</i> -beam	4×10^{-7}	room	$\langle 100 \rangle$	15	0.2, one
						0.4, one
						0.6, one
Al 5056	sputter	Ar: 1×10^{-2}	room	$\langle 100 \rangle$	12	0.5, one
Ti	<i>e</i> -beam	6×10^{-7}	room	$\langle 111 \rangle$	3	0.1, both
Cu	<i>e</i> -beam	2×10^{-6}	room	$\langle 111 \rangle$	6	0.1, both

described here were done in the MOS area of the Cornell Nanofabrication Facility and were preceded by a stringent RCA cleaning, as described in Ref. [34], in order to avoid any contamination of the silicon which is known to occur during annealing under regular clean laboratory conditions. The annealing process in the MOS area will be referred to in the following as “MOS-cleaned-and-annealed.”

In metals, heat is carried by both electrons and phonons. For bulk metals, it is therefore difficult to accurately obtain, from standard thermal conductivity experiments, the phonon contribution separately from the electron contribution to the total heat transport. Our thermal method, as applied to metal films, has the advantage of solely determining the phonon heat transport in the form of a phonon mean free path in the film. It must be emphasized that the metal films in this investigation act primarily as phonon scatterers rather than as heat conductors because of their thickness relative to the substrate thickness. At low temperatures, most of the heat in normal metals is carried by electrons. This thermal conductivity can be calculated using the law of Wiedemann-Franz-Lorenz (reviewed in Ref. [35]) and an appropriate electrical resistivity. Because heat transport is parallel to the film-substrate interface, the amount of heat carried by the film or the substrate depends on the thermal resistance of the film or the substrate. To calculate the thermal resistance, one multiplies the inverse of the thermal conductivity of the film (or substrate) by the length of the film (or substrate) divided by the cross-sectional area of the film (or substrate). Since the film and substrate have the same

length and width and differ only in thickness, a comparison of the thermal conductivity of the film multiplied by its thickness with the thermal conductivity of the substrate multiplied by its thickness is enough to determine which carries most of the heat. Fig. 1 shows the measured thermal conductivity of the polished, high purity 300 μm thick Si substrate multiplied by its thickness

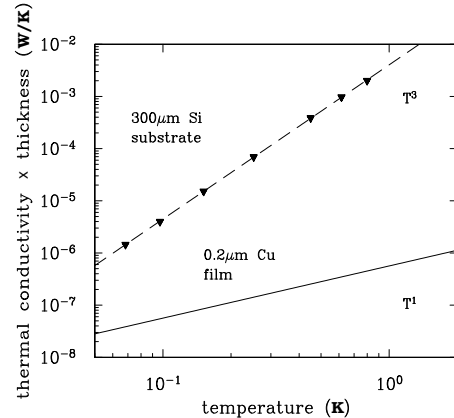


FIG. 1. The thermal conductivity of a high purity Si substrate (large faces polished and thin faces sandblasted, see Appendix) multiplied by its thickness, 300 μm : solid triangles; and the electronic thermal conductivity of a Cu film multiplied by its thickness, 0.2 μm : solid line. The solid triangles are actual measured data while the solid line is calculated as discussed in the text. The dashed line is a guide to the eyes. At 50 mK, only about 5% of the heat is carried in the film (by electrons); at higher temperatures, the percentage drops as T^{-2} .

(solid triangles). Fig. 1 also shows the thermal conductivity of a Cu film multiplied by its thickness, $0.2 \mu\text{m}$ (solid line), calculated as follows. Using a room temperature electrical resistivity of Cu of $1.56 \times 10^{-6} \Omega\text{cm}$ given in Ref. [36] and a residual resistivity ratio of 2 given in Ref. [4], the low temperature electrical resistivity is determined and used with the Wiedemann-Franz-Lorenz law to yield the low temperature thermal conductivity of the Cu film. Fig. 1 shows that almost all of the heat is carried by the substrate and very little heat is carried by the film, primarily because the thickness of the substrate is so much greater than that of the film. The same is true for the other metal films studied in this work, even more so when they become superconducting in the temperature range investigated here.

TABLE II. Comparison of the free surface RMS roughness as determined by AFM measurements with the dominant thermal phonon wavelength λ_{dom} at 1 K based on the Debye speed of sound, v_D , for the thin film samples studied.

film thickness (μm)	v_D^a (10^5 cm/s)	λ_{dom} at 1 K (\AA)	RMS Roughness (\AA)
<i>a</i> -Si	0.5	4.62	510
MBE Si	0.4	5.93	650
CaF ₂	0.1	4.10	450
MBE CaF ₂	0.4	4.10	450
Al	0.2	3.42	370
	0.4	3.42	370
	0.6	3.42	370
Al 5056	0.5	3.42	370
Ti	0.1	3.48	380
Cu	0.1	2.78	300
			10

^a Taken from Ref. [37] or estimated using Eq. 6 with v_t listed in Table III.

Since we are primarily interested in the thermal phonon mean free path in the film, $\ell_{\text{film(HC)}}$, we would like to minimize phonon scattering at the film-substrate interface and at the free surface of the film. Since the film-substrate interface is expected to be much smoother than the free surface of the film, we first consider the free surface roughness of the films studied in this work. Table II presents the root-mean-square (RMS) roughness of the free surfaces of the films studied as determined by atomic force microscopy (AFM) measurements at Cornell Center for Materials Research. Table II also presents the dominant thermal phonon wavelength at 1 K based on the Debye speed of sound of the materials listed. The wavelength of the thermal phonons is the relevant length. As can be seen, the RMS roughness is small compared to the length scale of the thermal phonons; and so, the free surfaces of the films should have little effect on the over-

all scattering of thermal phonons and thus on the overall conclusions of this work. In section III C, we will show experimental evidence by studying films thickness dependence that phonon scattering at the surfaces/interfaces is indeed negligible relative to that in the films.

The Monte Carlo (MC) simulations used to extract $\ell_{\text{film(HC)}}$ from the measurements has been described before [3]. Here, we mention briefly that additional scattering mechanisms such as scattering from free surface roughness can be included in the simulations, should that become necessary. For those who wish to determine $\ell_{\text{film(HC)}}$ (from heat conduction measurements below 1 K) without having to resort to performing their own simulations, we provide information in the Appendix, using the results of our MC simulations on a film-substrate sample with dimensions as typically used in our work.

In addition to extracting the phonon mean free path in a film, $\ell_{\text{film(HC)}}$, from thermal measurements of the film-substrate samples [3], we can predict $\ell_{\text{film(TM)}}$ from elastic measurements of the film-substrate samples if we assume that the film has the low energy excitations that are common in amorphous solids (and no other scattering centers). In the present work, the low-temperature internal friction of thin films is measured with double-paddle oscillators vibrating in their antisymmetric mode at $\sim 5.5 \text{ kHz}$ as described previously [38,39]. Thin films increase the internal friction of the paddle oscillator, Q_{paddle}^{-1} . From this, the internal friction of the film, Q_{film}^{-1} , is determined by [38]

$$Q_{\text{film}}^{-1} = \frac{G_{\text{sub}} t_{\text{sub}}}{3G_{\text{film}} t_{\text{film}}} (Q_{\text{paddle}}^{-1} - Q_{\text{sub}}^{-1}), \quad (1)$$

where t and G are thicknesses and shear moduli of substrate and film, respectively, and Q_{sub}^{-1} is the internal friction of the bare paddle (including the mounting losses). G_{film} is assumed to be equal to that of the bulk material [4,38]. The specific model used to obtain the phonon mean free path of a film, $\ell_{\text{film(TM)}}$, from the internal friction of a film is the tunneling model, originally proposed by Anderson, et al. [40], and independently by Phillips [41], expanded for elastic measurements by Jäckle [42]. The tunneling model connects the thermal phonon mean free path in a solid, ℓ , with the internal friction plateau of the solid, Q_0^{-1} , as follows. From Ref. [7], the expression for the thermal conductivity Λ is

$$\Lambda = \frac{1}{3} C_v v_D \ell = \frac{2.66 k_B^3}{6\pi\hbar^2} \frac{\pi}{2Q_0^{-1} v_t} T^2 \quad (2)$$

where, in the gas-kinetic picture, C_v is the low temperature specific heat per unit volume, v_D is the Debye speed of sound, k_B is Boltzmann's constant, \hbar is Planck's constant, v_t is the transverse speed of sound, and T is the temperature. Note that

$$Q_0^{-1} = \frac{\pi}{2} \left[\frac{\bar{P} \gamma_t^2}{\rho v_t^2} \right], \quad (3)$$

where \overline{P} is the uniform spectral density of the tunneling states, γ_t is their coupling energy to transverse phonons, and ρ is the mass density. Substituting for C_v within the Debye model of the phonon spectrum [43], Eq. 2 becomes

$$\ell = (1.43 \times 10^{-12} [\text{s K}]) \frac{v_D}{Q_0^{-1}} T^{-1} \quad (4)$$

or

$$\ell = (1.59 \times 10^{-12} [\text{s K}]) \frac{v_t}{Q_0^{-1}} T^{-1}, \quad (5)$$

assuming the empirical relation [37,44]

$$v_t \simeq 0.9 v_D, \quad (6)$$

where $[\text{s K}]$ are units of second and Kelvin. These equations provide the means to predict (within the tunneling model) what the phonon mean free path in a film ($\ell_{\text{film(TM)}}$) should be if the internal friction plateau of the film ($Q_0^{-1}_{\text{film}}$) is known. To repeat, Eq. 5 assumes that the internal friction plateau is due to the presence of glassy states in the film, and that no defects other than the glass-like excitations scatter the thermal phonons. The validity of these assumptions will be tested for the films investigated here by comparing $\ell_{\text{film(HC)}}$ with $\ell_{\text{film(TM)}}$.

III. RESULTS AND DISCUSSION

A. Silicon Films

Since we are searching for tunneling states in thin films, we started with *e*-beam *a*-Si, a film known to have such states [38], and will compare it with a film expected to be more structurally perfect. For this, we chose a crystalline silicon film produced by MBE which is expected to be very highly ordered. Fig. 2 shows the internal friction of a silicon double paddle oscillator with clean, polished surfaces, called “background,” and of the same kind of oscillator carrying these films. The internal friction resulting from the MBE film is negligible, as one might expect. In contrast to this, deposition of an *e*-beam *a*-Si film leads to a considerable increase of the internal friction above the background. The MBE Si was measured only in the annealed state, while the *e*-beam *a*-Si was measured in both as-deposited and annealed states. From the internal friction of the paddle carrying these *a*-Si films, Q_{paddle}^{-1} , the internal friction of the film itself, Q_{film}^{-1} , can be determined, using Eq. 1. In Fig. 3, Q_{film}^{-1} of these films is compared to that of bulk *a*-SiO₂ (see Ref. [7]). The annealing of the *e*-beam film causes almost a tenfold reduction in Q_{film}^{-1} , while the Q_{film}^{-1} of the annealed MBE film is too small to be determined. Table III lists the internal friction plateau $Q_0^{-1}_{\text{film}}$, the transverse speed of sound v_t , and the calculated thermal

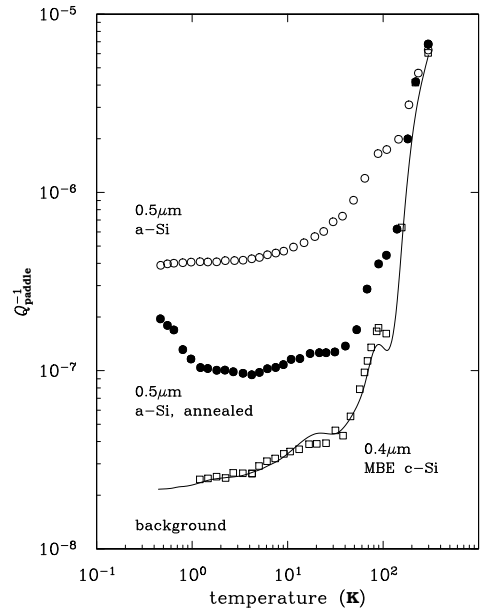


FIG. 2. The internal friction of a bare high purity silicon double-paddle oscillator (solid curve “background”) and of such paddles carrying *e*-beam *a*-Si and MBE Si films on the polished silicon surface. Note the negligible effect of the MBE film. The annealing of the *e*-beam *a*-Si film was done at 700°C for 1 hr under the MOS-cleaned-and-annealed condition (see text). The MBE Si film had been annealed at 850°C for 20 min in the process of manufacturing the oscillator (see text).

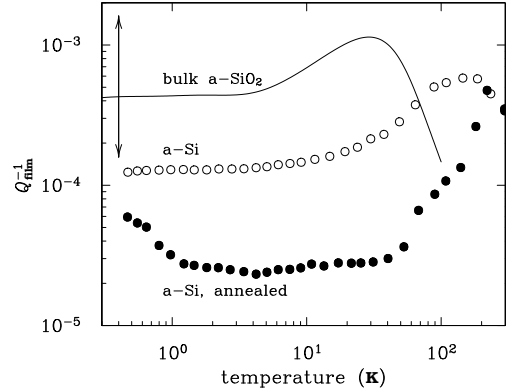


FIG. 3. Internal friction of an *e*-beam *a*-Si film, before and after annealing, compared to that of bulk *a*-SiO₂ (solid curve). The bulk *a*-SiO₂ data, measured at 4.5 kHz, is taken from J.E. Van Cleve, Ph.D. thesis, Cornell, published in Ref. [8]. The double-headed vertical arrow indicates the range of the temperature-independent internal friction plateau, measured on a wide range of bulk amorphous solids as reviewed in Ref. [7].

phonon mean free path $\ell_{\text{film(TM)}}(T)$ as function of temperature T given by Eq. 5, for *e*-beam *a*-Si and MBE Si. This table also contains the same information for the other films to be discussed below.

TABLE III. The internal friction plateau Q_0^{-1} film, the transverse speed of sound v_t , and the thermal phonon mean free path $\ell_{\text{film(TM)}}(T)$ predicted by Eq. 5.

	Q_0^{-1} film	v_t (10^5 cm/s)	$\ell_{\text{film(TM)}}(T)$ (μm)
a-Si	1.3×10^{-4}	4.16 ^b	$50.9/T$
MBE Si	negligible	5.33 ^c	e
CaF ₂	6.0×10^{-5}	3.69 ^c	$97.8/T$
Al	1.0×10^{-4} ^a	3.04 ^c	$48.3/T$
Al 5056	1.0×10^{-5} ^a	3.04 ^c	$483.4/T$
Ti	2.0×10^{-4} ^a	3.13 ^d	$24.9/T$
Cu	5.3×10^{-4} ^a	2.50 ^c	$7.5/T$

^a Taken from Ref. [4]

^b Taken from Ref. [38]

^c Taken from Ref. [44]

^d Taken from Ref. [45]

^e There is no Q_0^{-1} film value for the MBE Si film because the internal friction of this film was not detectable (see Fig. 2), and hence $\ell_{\text{film(TM)}}$ is expected to be very long.

Fig. 4 shows the measured phonon mean free path $\ell_{\text{film(HC)}}$ in the film as a function of temperature for the 0.5 μm thick *e*-beam *a*-Si film (solid circles) obtained from the heat conduction measurements. The dotted line represents the calculated phonon mean free path $\ell_{\text{film(TM)}}$ as predicted from Q_0^{-1} film of the *e*-beam *a*-Si (see Fig. 3, Table III), using the tunneling model as described in Section II. The measured $\ell_{\text{film(HC)}}$ is significantly smaller than $\ell_{\text{film(TM)}}$ which assumes scattering by tunneling states alone. Evidently, $\ell_{\text{film(HC)}}$ cannot be used to test for the existence of glassy excitations in this film. In addition to the tunneling states, other scattering centers must be present. The situation may be similar to *e*-beam *a*-SiO₂ films in which the additional scattering was explained by cracks or voids [3]. It is well known that *a*-Si films produced by *e*-beam evaporation contain similar defects [46–48].

Also shown in Fig. 4 is the measured $\ell_{\text{film(HC)}}$ for a 0.4 μm thick MBE Si film before annealing (solid squares). Very surprisingly, the phonon scattering in this film is also very large. Chemical impurities are unlikely as scatterers for the following reasons. (i) No evidence for such scattering was observed on bare silicon samples from the same batch as used in these experiments [3]. According to the SIMS analysis, only oxygen exists in the film at a concentration greater than in the substrate. But even the approximately tenfold increase of oxygen in the MBE film should not lead to a noticeable decrease of the experimental mean free path ℓ (defined in the Appendix, Eq. 7), and thus to a decrease of $\ell_{\text{film(HC)}}$ given the relatively small thickness of the film, unless the oxygen in the film somehow acts as a much stronger scattering center.

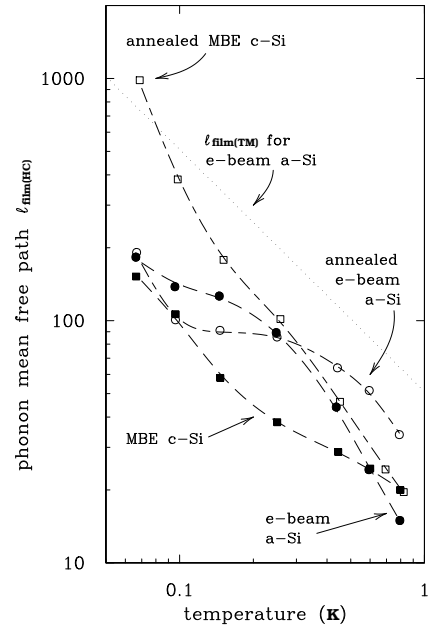


FIG. 4. Phonon mean free path $\ell_{\text{film(HC)}}$ of as-deposited and annealed silicon films. As-deposited *e*-beam *a*-Si: solid circles; annealed (700°C, 1 hr) *e*-beam *a*-Si: Open circles; as-deposited MBE Si: solid squares; annealed MBE Si (500°C, 1 hr followed by 700°C, 1.5 hrs): Open squares. The dotted line is $\ell_{\text{film(TM)}}(T)$, the tunneling model prediction based on the internal friction plateau of the as-deposited *e*-beam *a*-Si. Dashed lines are guides for the eyes.

(ii) Phonon scattering in oxygen-doped silicon has been found to depend on heat treatment [49,50] at frequencies in excess of ~ 300 GHz. However, phonons in this frequency range carry heat predominantly above 3 K, and no evidence exists for phonon scattering by oxygen at lower frequencies ($T < 1$ K).

In an attempt to detect any evidence for structural disorder in this film, an x-ray diffraction (XRD) analysis on the MBE Si sample was performed by M. Sardela and D. Cahill at the University of Illinois (Champaign-Urbana). High resolution open-detector scans around the Si(004) peak showed no difference between measurements conducted on the film side and on the substrate side of the *c*-Si film-substrate sample. Full width at half maximum values were found to be almost identical and no diffuse scattering or any disorder feature in the measurements of the film side was seen. In addition, a triple axis reciprocal space map around the Si(004) peak on the film side also could not detect any diffuse distribution nor asymmetry of the Si peak. These observations speak against the existence of grains with different orientations which might cause the phonon scattering. The near T^{-1} temperature dependence may be suggestive of scattering by sessile dislocations as reported, for example, by Wasserbäch in plastically deformed bulk copper, niobium, and tantalum [18]. If we assume that the cou-

pling between dislocations and phonons is similar, the dislocation density in the MBE film would have to range between 10^{10} and 10^{13} cm $^{-2}$, which seems rather high for MBE silicon. At this point, no search for dislocations in this MBE film has been undertaken.

MOS-cleaning-and-annealing of the MBE film as described above leads to an increase of $\ell_{\text{film(HC)}}$ shown in Fig. 4, most notably at the lower temperatures, although it remains below the mean free path predicted even for *e*-beam *a*-Si, except at the lowest temperature (see the dotted line, $\ell_{\text{film(TM)}}$, for *e*-beam *a*-Si based on the measured internal friction in Fig. 4). Thus, noticeable disorder remains even in the annealed MBE Si film. Internal friction was measured on the MBE Si film only after the MOS-cleaned-and-annealed process (heating to 850°C for 20 min as required for deposition of the silicon-nitride film, as described in Section II). The data, shown in Fig. 2, give no evidence for any low energy excitations. Thus, the only firm conclusion we can draw at this point is that the defects in the MBE film are not glass-like.

On the *e*-beam *a*-Si, the effect of crystallization on internal friction and phonon scattering was studied after annealing at 700°C for 1 hr which, according to Ref. [51], leads to almost complete crystallization. This was confirmed by the internal friction in Fig. 3 which decreased by almost one order of magnitude in the plateau regime, indicating that $\sim 90\%$ of the low energy excitations had disappeared. Below 1.0 K, however, the internal friction increased, indicative of a contamination shown to occur in *c*-Si annealed under all but the most stringent conditions (the MOS-cleaned-and-annealed process, as described in Ref. [34]). Very surprisingly, in the present experiment, even though the sample had been annealed under these stringent conditions, it seems to show contamination. The only explanation we can offer is that an impurity was trapped on the clean substrate surface during mounting in the *e*-beam evaporator which is located outside the MOS area. This impurity, trapped underneath the *a*-Si film, survived the MOS cleaning and led to the contamination during the annealing. Heat conduction below 1.0 K on such an annealed sample revealed only a small increase of $\ell_{\text{film(HC)}}$ above 0.3 K and even a decrease below that temperature, see Fig. 4. This change of $\ell_{\text{film(HC)}}$ upon annealing is interpreted as resulting from a combination of a decreased scattering by the smaller number of tunneling states, an increased scattering by the contaminants, and possibly a change in scattering from the defects of unknown nature which had been noticed already in the film prior to annealing. Obviously, these results cannot be used to extract any knowledge about the annealing of these unknown defects. They do, however, provide further evidence for the presence of the contaminants introduced into crystalline silicon during annealing under all but the most stringent conditions, thus further emphasizing the need for their identification and control.

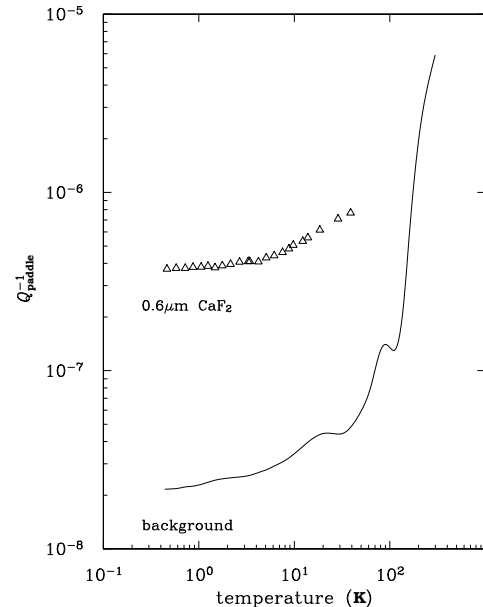


FIG. 5. The internal friction of a bare high purity silicon double-paddle oscillator (solid curve “background”) and of such a paddle carrying the *e*-beam CaF₂ film on the polished silicon surface. Note that the substrate orientation for the internal friction measurements is ⟨100⟩ while for the heat conduction measurements, the substrate orientation is ⟨111⟩, see Table I.

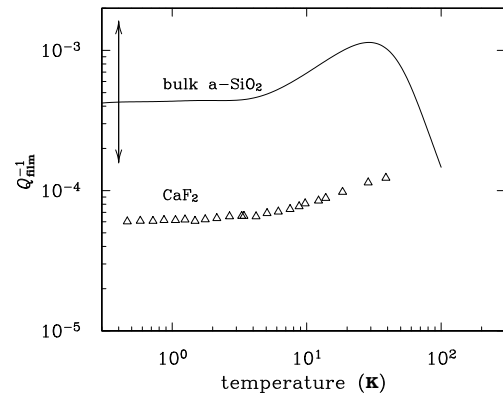


FIG. 6. Internal friction of the *e*-beam CaF₂ film compared to that of bulk *a*-SiO₂ (solid curve). The bulk *a*-SiO₂ data, measured at 4.5 kHz, is taken from J.E. Van Cleve, Ph.D. thesis, Cornell, published in Ref. [8]. The double-headed vertical arrow indicates the range of the temperature-independent internal friction plateau, measured on a wide range of bulk amorphous solids as reviewed in Ref. [7].

B. CaF₂ Films

As was just shown, crystalline films produced by crystallizing *a*-Si or by MBE deposition show little or no

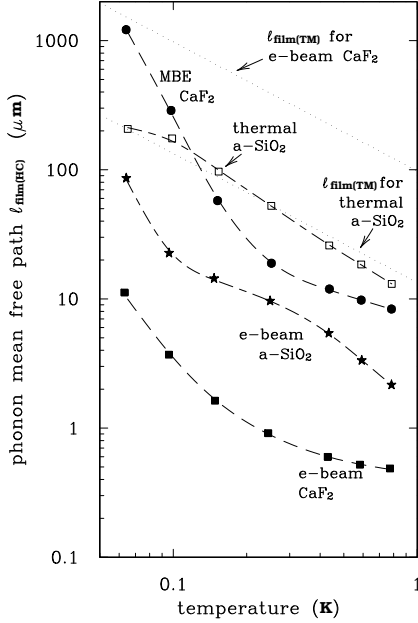


FIG. 7. Phonon mean free path $\ell_{\text{film(HC)}}$ of two different CaF_2 films. MBE CaF_2 : solid circles; e -beam CaF_2 : solid squares. The dotted lines are the tunneling model prediction based on internal friction measurements for e -beam CaF_2 and for thermal $a\text{-SiO}_2$, respectively. Data for the thermal (open squares) and e -beam (solid stars) $a\text{-SiO}_2$ films are taken from Ref. [3]. For thermal $a\text{-SiO}_2$, good agreement is shown between $\ell_{\text{film(HC)}}$ and $\ell_{\text{film(TM)}}$, which had also been found in ion-implanted silicon [9], as mentioned in the Introduction. Dashed lines are guides for the eyes.

evidence for tunneling states in low temperature internal friction. It is therefore surprising that a $0.6 \mu\text{m}$ thick film of crystalline e -beam CaF_2 increases the damping of the double paddle oscillator by over one order of magnitude, see Fig. 5. The internal friction of the film itself is compared with that of $a\text{-SiO}_2$ in Fig. 6. It is nearly temperature independent and close to the range found for all amorphous solids studied to date (with the exception of certain hydrogenated $a\text{-Si}$ films, as discussed in Ref. [38]). Thus, the large internal friction observed previously in polycrystalline metal films [4] apparently also occurs in some crystalline dielectric films. Assuming that its cause is glass-like excitations, we can again predict an $\ell_{\text{film(TM)}}$ for the CaF_2 film, shown as the dotted line in Fig. 7. The measured $\ell_{\text{film(HC)}}$ for this CaF_2 film is far smaller than predicted. In another CaF_2 film which had been deposited at a higher temperature by MBE to improve its structure, its $\ell_{\text{film(HC)}}$, though larger than for the first one, is still smaller even than that measured on a thermal $a\text{-SiO}_2$ film in which the phonon scattering is determined solely by the glassy excitations and its $\ell_{\text{film(HC)}}$ agrees perfectly with that of the TM's prediction (see Ref. [3] for details). Nonetheless, $\ell_{\text{film(HC)}}$ for the latter CaF_2 film seems closer to that of a

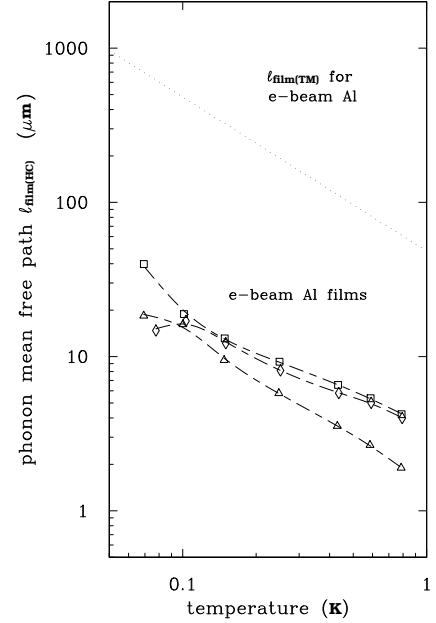


FIG. 8. Phonon mean free path $\ell_{\text{film(HC)}}$ for e -beam Al films that are $0.2 \mu\text{m}$ (open triangles), $0.4 \mu\text{m}$ (open squares), and $0.6 \mu\text{m}$ (open diamonds) thick. The dotted line is the tunneling model prediction based on internal friction (see Table III). Dashed lines are guides for the eyes.

macroscopically as well as microscopically disordered amorphous film, like e -beam $a\text{-SiO}_2$, as also shown in Fig. 7. There is, however, no convincing evidence for glass-like excitations in this CaF_2 film. Like in the e -beam $a\text{-Si}$ film, some unknown scattering process masks the effect of the glass-like excitations, if they exist at all.

C. Metal Films

Fig. 8 shows $\ell_{\text{film(HC)}}(T)$ for three e -beam Al films, 0.2 , 0.4 , and $0.6 \mu\text{m}$ thick. The absence of any significant dependence on the film thickness validates the assumption used in our analysis that the scattering occurs predominantly within the films and not at the interfaces, an assumption which so far had been based only on the smoothness observed on the free surfaces as listed in Table II. The dotted line is the prediction for $\ell_{\text{film(TM)}}(T)$ based on the internal friction of the e -beam Al film reported earlier [4] (see also Table III). As for the two previous examples, the observed phonon scattering far exceeds the scattering expected on the basis of the tunneling model.

In Ref. [4], it had been shown that the low temperature internal friction of an Al film on a Si substrate was very similar to that of heavily deformed bulk Al. It was therefore interesting to compare the phonon mean free path in the film with that observed in heavily deformed bulk Al.

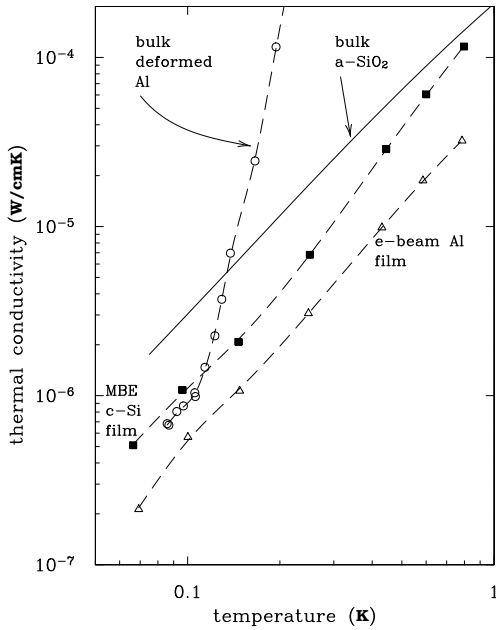


FIG. 9. The measured thermal conductivity of bulk 5% deformed 5N Al and bulk a - SiO_2 along with the phonon thermal conductivity of MBE Si and e -beam Al films converted from their phonon mean free path. For the bulk deformed Al, there is an electronic contribution to the thermal conductivity which seems to be completely frozen out below 0.1 K, leaving only the phonon thermal conductivity. The MBE Si film seems to have defects comparable to those of bulk deformed Al, at least below 0.1 K. The bulk a - SiO_2 data (solid curve) are taken from Ref. [52].

For that purpose, a 5N purity Al rod, 2.5 mm in diameter, was first annealed at 560°C and subsequently stretched by 5%. Its thermal conductivity is shown in Fig. 9 along with that of bulk a - SiO_2 , typical for an amorphous solid. The thermal conductivity of the deformed bulk Al above 0.1 K is dominated by electrons. However, below that temperature, the heat is expected to be carried predominantly by the lattice. The phonon thermal conductivity of the film, as calculated from the phonon mean free path $\ell_{\text{film}(\text{HC})}$ (shown in Fig. 8), is also shown in Fig. 9. Above 0.1 K, the two curves show the difference between the heat transport by phonons and electrons, and by the phonons alone, separated here experimentally for the first time. Below 0.1 K, the phonon thermal conductivity (derived from the measured $\ell_{\text{film}(\text{HC})}$) is very close to that measured on the bulk sample. This suggests that the defects which scatter the phonons in the film are very similar to those in the heavily deformed bulk sample. The same conclusion had been reached previously in internal friction measurements, where the internal friction of bulk Al approaches that of e -beam Al film with plastic deformation [4]. The defects causing the internal friction had been tentatively identified as dislocations or dislocation kinks. It is tempting to suggest that the thermal

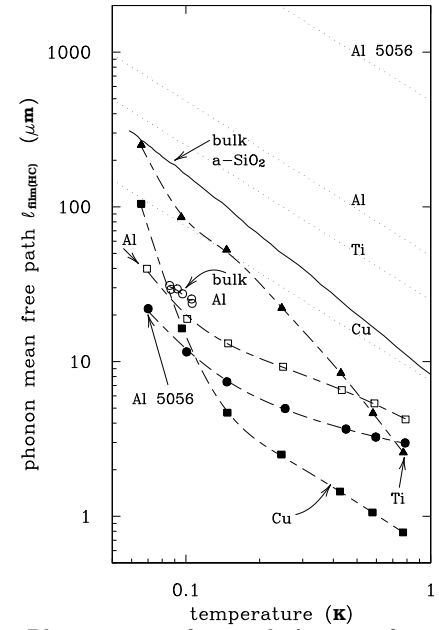


FIG. 10. Phonon mean free path $\ell_{\text{film}(\text{HC})}$ for a bulk sample of 5% deformed 5N Al: open circles; for a 0.4 μm thick e -beam Al film: open squares; for a 0.5 μm thick sputtered alloy Al 5056 film: solid circles; for a 0.1 μm thick e -beam Ti film: solid triangles; and for a 0.1 μm thick e -beam Cu film: solid squares. The labelled dotted lines are tunneling model predictions of $\ell_{\text{film}(\text{TM})}$ based on internal friction measurements (see Table III). The solid curve is the phonon mean free path in bulk a - SiO_2 taken from Ref. [52]. Dashed lines are guides for the eyes.

phonons in the films are also scattered by these defects. However, a close connection between the defects scattering the thermal phonons and those leading to the internal friction (a relaxational process) is unlikely, for the following reason. The alloy Al 5056 in bulk form has an exceptionally small low temperature internal friction, even as a sputtered film (Table III). This has been explained by dislocation pinning [4]. The phonon mean free path $\ell_{\text{film}(\text{HC})}$ in this film, however, is still close to that of all other metal films, see Fig. 10. It follows that if dislocations are responsible for both the internal friction and the thermal phonon scattering in the metal films and in the deformed bulk Al, the mechanisms by which they influence the thermal phonon scattering and the internal friction must be different. Also shown in Fig. 9 is the phonon thermal conductivity of MBE Si converted from its phonon mean free path, which seems to have defects comparable to that of bulk deformed Al.

A comparison between measured and predicted phonon mean free paths ($\ell_{\text{film}(\text{HC})}$, $\ell_{\text{film}(\text{TM})}$) is shown in Fig. 10 for four metal films (Al, alloy Al 5056, Ti, Cu), with the phonon mean free path of a - SiO_2 for comparison. The apparent lack of correlation between $\ell_{\text{film}(\text{HC})}$ and $\ell_{\text{film}(\text{TM})}$ enable us to generalize the same conclusion to

other metallic films, which is, if glass-like lattice vibrations exist in them, their effect is masked by the unknown defects. Most remarkably, the phonon scattering in the alloy Al 5056 is not different at all from that in the other metallic films, even though the density of tunneling states in this alloy film is at least one order of magnitude smaller than in $a\text{-SiO}_2$, based on the internal friction measurements.

As observed in internal friction [4], the measured $\ell_{\text{film(HC)}}$ is unaffected by superconductivity (T_c is 0.4 K for Ti, 0.92 for alloy Al 5056 [53], and 1.2 K for Al,). It is concluded that phonon scattering by electrons is unimportant. Klemens has derived an expression for the phonon-electron scattering coefficient P in terms of the electron-phonon scattering coefficient E [54]. Using the value for E measured by Berman and MacDonald for pure copper [55,56], we calculate an ℓ_{film} (of phonons being scattered by electrons) at 1 K to be $\sim 15 \mu\text{m}$. This phonon scattering rate (due to electrons) is more than an order of magnitude less than the phonon scattering rate observed in Fig. 10 for the Cu film. Note that the calculation of $15 \mu\text{m}$ should not be taken too seriously as its assumptions [57] of the adiabatic principle, of a phonon Debye spectrum, and of a free electron gas may not be adequate at these temperatures for a thin polycrystalline Cu film with a residual resistivity ratio of 2 [4]. Nevertheless, this estimate agrees with our observation that electron-phonon interaction is not significant in our experiment.

IV. CONCLUSIONS

Measurements of the thermal phonon mean free path on films of amorphous and MBE Si, of polycrystalline and MBE CaF_2 , of pure metallic Al, Cu, and Ti, and of the metallic alloy Al 5056 below 1.0 K have revealed, in all cases, similar strong phonon scattering. Scattering by surface and interface roughness can be excluded, since nearly the same thermal phonon mean free path $\ell_{\text{film(HC)}}$ has been observed in Al films of different thicknesses. In searching for the origin of this phonon scattering, we have also measured the low temperature internal friction of the Si and CaF_2 films (that of the metal films had been measured previously, Ref. [4]) and also the thermal conductivity of a bulk Al rod after a 5% plastic elongation. In all cases, $\ell_{\text{film(HC)}}$ was found to be much smaller than the expected mean free path $\ell_{\text{film(TM)}}$ based on the internal friction and assuming that the defects are glass-like. The discrepancy is particularly striking for the MBE Si film in which no internal friction was observed, yet $\ell_{\text{film(HC)}}$ was similar to that found in all other films. In this case, the phonon scattering is particularly puzzling since the film is expected to be structurally more perfect. In all other films, macroscopic defects like grain boundaries, voids, cracks, or dislocations may be the cause for the phonon

scattering. In the deformed bulk Al, the phonon mean free path was found to be equal to that in thin Al films. Since in the bulk sample, individual dislocations or aggregates thereof are likely phonon scatterers, they may also be the cause for the scattering in the films. However, dislocation motion, presumably tunneling, which has been invoked to explain the internal friction of deformed Al and of Al films (see Ref. [4,58]) is an unlikely cause for the thermal phonon scattering since the same $\ell_{\text{film(HC)}}$ in Al was also found in the alloy Al 5056, in which dislocation motion appears to be suppressed, resulting in a greatly reduced internal friction. In conclusion, both internal friction and phonon scattering have been shown to be sensitive probes for thin film disorder, including that in MBE Si. The nature of such disorder and the mechanisms by which it affects the elastic and thermal properties are as yet not known. No evidence for the existence of glass-like lattice vibrations has been detected.

Acknowledgements

We gratefully acknowledge the help of Aaron Judy with the AFM measurements, Glen Wilk in preparing the MBE Si film at Texas Instruments (Dallas), and Ken Krebs in fabricating the MBE CaF_2 film at the University of Georgia (Athens) and in providing very useful information on that film's defects. We thank Mauro Sardela and David Cahill for XRD analysis at the University of Illinois (Champaign-Urbana) and Bob Reedy for the SIMS investigation of the MBE Si film at the National Renewable Energy Laboratory. We also thank R.S. Crandall for fruitful discussions. This work was supported by the National Science Foundation, Grant No. DMR-9701972 and the National Renewable Energy Laboratory, Grant No. RAD-8-18668. Additional support was received from the Cornell Nanofabrication Facility, NSF Grant No. ECS-9319005, and the Cornell Center for Materials Research.

Appendix

The technique used in this investigation for the measurement of the thermal phonon mean free path in thin films has been described before [3]. Although the experimental schematic resembles that of a thermal conductivity measurement, see Fig. 11, it should be emphasized that our experiment leads directly to a thermal phonon mean free path, rather than to a thermal conductivity Λ , from which the mean free path ℓ has to be calculated using the gas-kinetic expression

$$\Lambda = \frac{1}{3} C_v \bar{v} \ell, \quad (7)$$

which requires knowledge of the specific heat C_v of the heat carrying excitations or phonons traveling with an

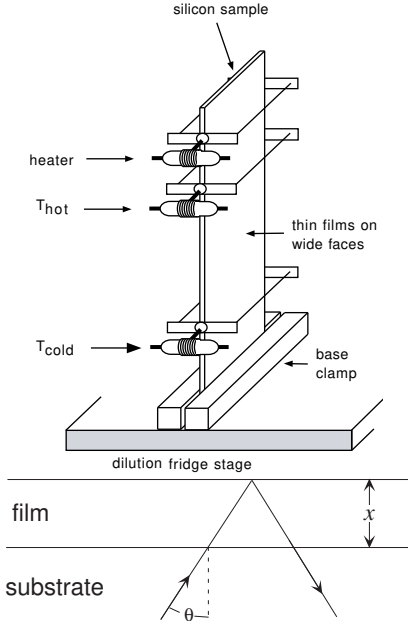


FIG. 11. Schematic of 1-D heat conduction experiment; the sample is cleaved from a high purity commercial silicon wafer (orientation $\langle 111 \rangle$ or $\langle 100 \rangle$) with both large faces polished; the thin faces are sandblasted as described in Ref. [3]. Also shown is a ballistic path of a thermal phonon from the silicon substrate through a thin film as modeled in the MC simulations.

average velocity \bar{v} . In amorphous solids, for example, this C_v cannot be measured. It can only be calculated from \bar{v} through the use of the Debye model.

The analysis of the heat conduction measurements on the silicon substrate carrying the film requires a Monte Carlo simulation which, though straightforward, is nonetheless time-consuming. By strictly adhering to the specifics as listed below (including sample and clamp geometry), one can extract the phonon mean free path in a film, ℓ_{film} (called $\ell_{\text{film(HC)}}$ in this paper), from ℓ_{exp} (the experimentally measured phonon mean free path of the film-substrate sample) without having to repeat any MC simulations, as will be shown in this Appendix.

Fig. 12 is a plot of the results of MC simulations on a film-substrate sample with dimensions typically used in this investigation. For any particular simulation, ℓ_{film}/x is an input parameter where x is the film thickness. The output parameter is ℓ_{MC} , a simulated phonon mean free path of the film-substrate sample. To determine ℓ_{film} , one sets an ℓ_{exp} equal to an ℓ_{MC} in Fig. 12 to find the corresponding ℓ_{film}/x ; multiplying by x then yields the desired value, ℓ_{film} , that directly corresponds to the measured ℓ_{exp} .

In order to use Fig. 12 as above, the film-substrate sample must be mounted as shown in Fig. 11. Furthermore, the four thin sides of the high purity silicon substrate must be completely roughened (by sandblasting,

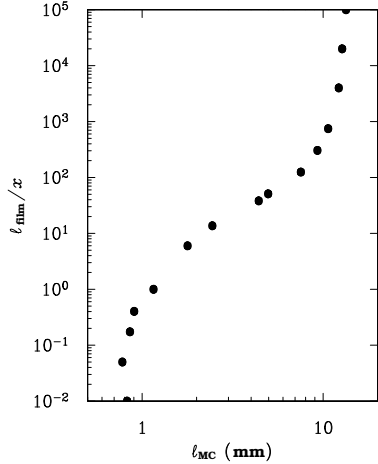


FIG. 12. Typical plot of ℓ_{film}/x versus ℓ_{MC} where x is the film thickness. Normalizing ℓ_{film} with respect to x allows the same plot to be used for different film thicknesses as long as the sample and clamp geometry has not changed (see text for details). The actual code of the Monte Carlo programs may be found in Ref. [59].

for example) while the two wide faces must be smooth from Syton polishing, for example), as explained in Ref. [3]. Any film of thickness x must cover both wide faces entirely and uniformly. The height of the sample above the top of the base clamp should be 44.5 mm, the width of the sample 7 mm, and the thickness of the substrate 0.279 mm. The height of the heater, cold thermometer, and hot thermometer clamp above the top of the base clamp should be 41 mm, 4 mm, and 25 mm, respectively. The two interfaces between the heater clamp and the sample (areas of contact) should each be of dimensions $0.279 \times 2 \text{ mm}^2$ while the four interfaces between the thermometer clamps and the sample should each be $0.279 \times 1.5 \text{ mm}^2$. The effect of varying these details are discussed in Ref. [3].

- [1] M. Ohring, *The Materials Science of Thin Films* (Academic Press, San Diego, 1992), ch.14.
- [2] D. E. Carlson and C. R. Wronski, *Appl. Phys. Lett.* **28**, 671 (1976).
- [3] P. D. Vu, J. R. Olson, and R. O. Pohl, *J. Low Temp. Phys.* **113**, 123 (1998).
- [4] X. Liu, E. J. Thompson, B. E. White, Jr., and R. O. Pohl, *Phys. Rev. B* **59**, 11767 (1999).
- [5] A. K. Raychaudhuri and R. O. Pohl, *Phys. Rev. B* **46**, 10657 (1992).
- [6] W. A. Phillips, *Rep. Prog. Phys.* **50**, 1657 (1987).
- [7] K. A. Topp and D. G. Cahill, *Z. Phys. B* **101**, 235 (1996).
- [8] P. A. Medwick, B. E. White, Jr., and R. O. Pohl, *J.*

Alloys and Compounds **270**, 1 (1998).

[9] X. Liu, P. D. Vu, R. O. Pohl, F. Schiettekatte, and S. Roorda, Phys. Rev. Lett. **81**, 3171 (1998).

[10] M. L. Roukes, M. R. Freeman, R. S. Germain, R. C. Richardson, and M. B. Ketchen, Phys. Rev. Lett. **55**, 422 (1985).

[11] J. F. DiTusa, K. Lin, M. Park, M. S. Isaacson, and J. M. Parpia, Phys. Rev. Lett. **68**, 1156 (1992).

[12] N. Giordano, W. Gilson, and D. E. Prober, Phys. Rev. Lett. **43**, 725 (1979).

[13] N. Giordano, Phys. Rev. B **22**, 5635 (1980).

[14] N. Perrin, Phys. Rev. B **48**, 12151 (1993).

[15] M. N. Wybourne, C. G. Eddison, and M. J. Kelly, J. Phys. C **17**, L607 (1984).

[16] C. G. Eddison and M. N. Wybourne, J. Phys. C **18**, 5225 (1985).

[17] I.-S. Yang, A. C. Anderson, Y. S. Kim, and E. J. Cotts, Phys. Rev. B **40**, 1297 (1989).

[18] W. Wasserbäch, Phys. Stat. Sol. **128**, 55 (1991).

[19] J. C. Hensel, R. T. Tung, J. M. Poate, and F. C. Unterwald, Phys. Rev. Lett. **54**, 1840 (1985).

[20] K. L. J. F. DiTusa, M. Park, M. S. Isaacson, and J. M. Parpia, Phys. Rev. Lett. **68**, 678 (1992).

[21] D. C. Ralph, A. W. W. Ludwig, J. von Delft, and R. A. Buhrman, Phys. Rev. Lett. **72**, 1064 (1994).

[22] V. Chandrasekhar, P. Santhanam, N. A. Penebre, R. A. Webb, H. Vloeberghs, C. V. Haesendonck, and Y. Bruynseraede, Phys. Rev. Lett. **72**, 2053 (1994).

[23] G. Zarand and A. Zawadowski, Phys. Rev. B **50**, 932 (1994).

[24] D. C. Ralph and R. A. Buhrman, Phys. Rev. B **51**, 3554 (1995).

[25] M. A. Blachly and N. Giordano, Phys. Rev. B **51**, 12537 (1995).

[26] H. von Löhneysen, Phys. Rep. **79**, 161 (1981).

[27] H. J. Guntherodt and H. Beck, eds., *Glassy Metals I* (Springer-Verlag, New York, 1981), p.167.

[28] H. von Löhneysen, Mat. Sci. Eng. **A133**, 51 (1991).

[29] The Czochralski-grown Si is commercially available from Virginia Semiconductor Inc. in Fredericksburg, Virginia, while the float-zone refined Si is a donation from Dr. Peter Wagner of Wacker Siltronic in Burghausen, Germany.

[30] N. S. Sokolov, N. L. Yakovlev, and J. Almeida, Solid State Commun. **76**, 883 (1990).

[31] K. Krebs, private communication.

[32] W. Kern, RCA Eng. **28**, 99 (1983).

[33] Recipe given by staff at the Cornell Nanofabrication Facility, Ithaca, New York, and dubbed "Piranha-etch".

[34] X. Liu, R. O. Pohl, S. Asher, and R. S. Crandall, J. Non-cryst. Solids **227-230**, 407 (1998).

[35] G. S. Kumar, G. Prasad, and R. O. Pohl, J. Mat. Sci. **28**, 4261 (1993).

[36] N. W. Ashcroft and N. D. Mermin, *Solid State Physics* (Saunders College, Philadelphia, 1976), p.21.

[37] T. Klitsner and R. O. Pohl, Phys. Rev. B **36**, 6551 (1987).

[38] X. Liu and R. O. Pohl, Phys. Rev. B **58**, 9067 (1998).

[39] C. L. Spiel and R. O. Pohl, Rev. Sci. Instr. (to be submitted).

[40] P. W. Anderson, B. I. Halperin, and C. M. Varma, Philos. Mag. **25**, 1 (1972).

[41] W. A. Phillips, J. Low Temp. Phys. **7**, 351 (1972).

[42] J. Jäckle, Z. Phys. B **257**, 212 (1972).

[43] N. W. Ashcroft and N. D. Mermin, *Solid State Physics* (Saunders College, Philadelphia, 1976), p.458.

[44] E. T. Swartz and R. O. Pohl, Rev. Mod. Phys. **61**, 605 (1989).

[45] R. C. Weast, ed., *CRC Handbook of Chemistry and Physics 67* (CRC Press, Inc., Boca Raton, Florida, 1986), p.E-43.

[46] D. Williamson, S. Roorda, M. Chicoine, R. Tabti, P. A. Stolk, S. Acco, and F. W. Saris, Appl. Phys. Lett. **67**, 226 (1995).

[47] J. S. Custer, M. O. Thompson, D. C. Jacobson, J. M. Poate, S. Roorda, W. C. Sinke, and F. Spaepen, Appl. Phys. Lett. **64**, 437 (1994).

[48] S. Roorda, W. C. Sinke, J. M. Poate, D. C. Jacobson, S. Dierker, B. S. Dennis, D. J. Eaglesham, F. Spaepen, and P. Fuoss, Phys. Rev. B **44**, 3702 (1991).

[49] G. Schrag, M. Rebmann, C. Wurster, F. Zeller, K. Lassmann, and W. Eisenmenger, Phys. Stat. Sol. (a) **168**, 37 (1998).

[50] F. Zeller, K. Lassmann, and W. Eisenmenger, Physica B **263-264**, 108 (1999).

[51] G. L. Olson and J. A. Roth, Mat. Sci. Rep. **3**, 1 (1988).

[52] R. C. Zeller and R. O. Pohl, Phys. Rev. B **4**, 2029 (1971).

[53] W. Duffy, Jr., J. Appl. Phys. **68**, 5601 (1990).

[54] P. G. Klemens, *Encyclopedia of Physics*, vol. 14, S. Flügge, ed., (Springer Verlag, Berlin, 1956) p. 198.

[55] R. Berman and D. K. C. MacDonald, Proc. Roy. Soc. **A211**, 122 (1952).

[56] P. Lindenfeld and W. B. Pennebaker, Phys. Rev. **127**, 1881 (1962).

[57] H. von Löhneysen and F. Steglich, Z. Phys. B **29**, 89 (1978).

[58] E. Thompson and R. O. Pohl, Mat. Res. Soc. Symp. Proc. **562** (1999), in press.

[59] P. D. Vu, *Phonon Scattering in Thin Films Below 1 K*, Ph.D. thesis, Cornell University (1999).